Phage-assisted evolution of botulinum neurotoxin proteases with reprogrammed specificity

Travis R. Blum[1,2,3], **Hao Liu**[4], **Michael S. Packer**[1,2,3], **Xiaozhe Xiong**[4], **Pyung-Gang Lee**[4], **Sicai Zhang**[4], **Michelle Richter**[1,2,3], **George Minasov**[5], **Karla J. F. Satchell**[5], **Min Dong**[4], **David R. Liu**[1,2,3]

[1]Merkin Institute of Transformative Technologies in Healthcare, Broad Institute of Harvard and MIT, Cambridge, MA, 02142

[2]Department of Chemistry and Chemical Biology, Harvard University, Cambridge, MA, 02138

[3]Howard Hughes Medical Institute, Harvard University, Cambridge, MA, 02138

[4]Department of Urology, Boston Children's Hospital, Department of Microbiology and Department of Surgery, Harvard Medical School, Boston, MA, 02115

[5]Department of Microbiology-Immunology, Northwestern University School of Medicine, Chicago, IL 60611

Abstract

While bespoke sequence-specific proteases have the potential to advance biotechnology and medicine, generating proteases with tailor-made cleavage specificities remains a major challenge. We developed a phage-assisted protease evolution system with simultaneous positive and negative selection, and applied it to three botulinum neurotoxin (BoNT) light-chain proteases. We evolved BoNT/X protease into separate variants that preferentially cleave VAMP4 and Ykt6, evolved BoNT/F protease to selectively cleave the non-native substrate VAMP7, and evolved BoNT/E protease to cleave PTEN but not any natural BoNT protease substrate in neurons. The evolved proteases display large changes in specificity (218- to >11,000,000-fold) and can retain their ability to form holotoxins that self-deliver into primary neurons. These findings establish a versatile platform for reprogramming proteases to selectively cleave new targets of therapeutic interest.

Supplementary Materials:
Materials and Methods
Figures S1-S25
Tables S1-S9
References (67–73)

One Sentence Summary:

Phage-assisted evolution reprograms botulinum neurotoxin proteases to selectively cleave proteins of biomedical interest *in vitro* and in neurons.

The ability of proteases to cleave protein targets with high efficiency and specificity enables them to play important roles in biology, biotechnology, and medicine (1). Applications of proteases would be greatly expanded by the ability to reprogram them to selectively cleave new targets for which no known protease exists. While proteases have been engineered or evolved for increased stability (2), solvent tolerance (3), inhibitor resistance (4, 5), activity (6–8), and altered specificity (9–15), reports of successfully changing substrate specificity beyond a single amino acid in the primary peptide recognition sequence are rare (16–19). Moreover, the laboratory evolution of proteins to accept new substrates commonly results in substrate promiscuity (19–27). While negative selections during protease evolution have reduced off-target activity for single amino acid substrate changes (28–33), the limits of directed evolution's ability to extensively reprogram proteases away from their original substrates to achieve highly specific cleavage of a new target remain largely untested.

Many pathogens have evolved proteases that cleave proteins with exquisite specificity to precisely modulate host-cell functions. These proteases, exemplified by botulinum neurotoxins (BoNTs), have proven to be powerful therapeutic agents. BoNTs are a family of bacterial toxins with seven major serotypes (BoNT/A to BoNT/G). Each BoNT consists of a heavy chain (HC, ~100-kDa) and a light chain (LC, ~50-kDa) connected through a disulfide bond (34, 35). The HC serves as a delivery vehicle, containing both receptor-binding and membrane translocation domains, while the LC is a zinc-dependent metalloprotease. BoNT HCs mediate entry into the neuronal cytosol, where disulfide bond reduction releases the LC. Known substrates of BoNT LCs are all members of the SNARE protein family, which mediates membrane fusion in eukaryotic cells (36). The LCs then target and selectively cleave SNARE proteins essential for synaptic vesicle exocytosis. BoNT/A, BoNT/C, and BoNT/E cleave the 25-kDa synaptosomal-associated protein (SNAP-25); BoNT/B, BoNT/D, BoNT/F and BoNT/G cleave vesicle-associated membrane proteins 1, 2, and 3 (VAMP1, VAMP2, and VAMP3); and BoNT/C also cleaves Syntaxin-1. Cleavage of these proteins blocks synaptic vesicle exocytosis, causing muscle paralysis. While commonly known for cosmetic applications, BoNTs have also been used as important therapeutic proteins for over 30 years to treat many other conditions (35).

The exquisite selectivity of BoNT LC proteases is critical for their therapeutic application. Past efforts to engineer BoNT LCs have expanded their ability to cleave homologous SNARE proteins, but have been unable to retarget these proteases to selectively cleave proteins that differ even modestly from their native substrates. For example, engineered BoNT/A and BoNT/E proteases cleave SNAP-23, but retain activity on SNAP-25 (37, 38). Due to their high specificity and dependence on multiple exosites and conformational changes to mediate substrate recognition and cleavage (39, 40), the prospect of reprograming BoNT proteases to cleave proteins beyond SNARE family members has seemed out of reach.

While several systems for protease evolution have been reported (41), phage-assisted continuous evolution (PACE) is especially well-suited to address this challenge since PACE continuously diversifies and selects gene variants with desired properties ~100-fold faster than stepwise protein evolution methods (5, 19, 21–24, 42–50). We recently reported a PACE selection for protein cleavage (5), and used the selection to evolve tobacco etch virus (TEV) proteases that cleave a sequence in human IL-23 (19). Because this PACE system did not enable selection against off-target cleavage activity, the evolved TEV protease maintained strong activity on its native substrate (19). A platform to generate highly selective proteases that avoid such promiscuity has been a longstanding goal (51, 52). Here, we developed a simultaneous PACE positive- and negative-selection system and used it to reprogram the substrate specificity of three BoNT LC proteases, yielding four proteases with high specificity for their new targets. These results establish a system to rapidly evolve a class of clinical proteases to preferentially cleave non-native targets.

Results

Development of a phage-assisted evolution negative selection for proteases

PACE uses a modified M13 bacteriophage that encodes an evolving gene of interest in place of *gIII*, which encodes a protein (pIII) essential for phage replication. During PACE, *gIII* is encoded on an accessory plasmid (AP) in *E. coli* host cells, and its expression is made dependent on the activity of interest (24, 50). To evolve proteases in PACE, we use a protease-activated RNA polymerase (PAP), an autoinhibited T7 (or T7 variant) RNA polymerase (RNAP) expressed in host cells as a fusion with its native inhibitor T7 lysozyme (enLys, Fig. 1A) (5). The linker between T7 RNAP and T7 lysozyme contains the proteolysis target sequence of interest. Cleavage of the target sequence releases T7 lysozyme, restoring T7 RNAP activity and triggering expression of *gIII*, which is under control of the T7 promoter (Fig. 1A). Propagating phage are continuously diluted by fresh host cells and are continuously mutated by induction of a host-cell mutagenesis plasmid (44).

We first verified that LC proteases from BoNT/E, BoNT/F, and the recently discovered BoNT-like toxin BoNT/X (34, 53, 54), could perform proteolytic activation of T7-PAPs containing minimized substrate fragments, resulting in luciferase expression. We observed that all three proteases are functional when expressed in *E. coli*, and activate T7-PAP in a manner consistent with their native cleavage specificities (fig. S1–S2).

Next, we developed a PACE negative selection that impedes the propagation of phage encoding proteases with off-target cleavage activities. We previously evolved a T7-RNA polymerase variant with high selectivity for the T3 promoter (T3'-RNAP) (21). We converted T3'-RNAP, which remains inhibited by tethered T7 lysozyme, into a protease-activated T3' polymerase (T3'-PAP) that supports positive selection through transcription of *gIII* in response to on-target cleavage (Fig. 1A). We then used a T7-PAP containing an off-target substrate to construct a negative selection in which off-target cleavage drives expression of *gIII-neg*, which encodes a dominant-negative pIII variant that suppresses phage replication (21), from the T7 promoter (Fig. 1A). Negative-selection stringency can be

tuned using ribosome binding site (RBS) variants to control translation rates of pIII-neg in different host strains.

To enable greater control of selection pressure when needed, we performed simultaneous positive and negative selection using phage-assisted non-continuous evolution (PANCE) (23, 46–48), in which phage are periodically, rather than continuously, diluted into media containing fresh host cells. PANCE is conducted in 96-well plates and offers reduced selection stringency in a high-throughput format. PANCE allows parallel protease evolution experiments at a range of negative-selection stringencies, while simultaneously maintaining high-stringency positive selection in all hosts.

Dual-selection PANCE evolves a Ykt6-selective BoNT/X protease

We started with BoNT/X, which is unique among BoNT family proteases in that it cleaves not only VAMP1, 2, and 3, but also VAMP4, 5, and Ykt6 (53, 54). While BoNT/X in principle could serve as a powerful tool to investigate the roles of VAMP4 and Ykt6 in cells, its substrate promiscuity impedes this possibility. To explore whether the selectivity of BoNT/X protease can be improved using dual-selection PANCE, we generated a library of mutant BoNT/X LC protease genes through propagation in host strains with the mutagenic plasmid MP6 (44), and inoculated this library into host strains each supporting high-stringency positive selection for Ykt6 cleavage alongside negative selection against VAMP1 cleavage at various selection stringencies (Fig. 1B top, 1C). Initial passages supported phage survival only at low stringency, enriching the mutation A166E. BoNT/X proteases containing A166E (for example, X(3206)A14) showed increased, though incomplete, preference for Ykt6 over VAMP1 (fig. S2). We then subjected the A166E-enriched population to additional PANCE in triplicate using the same set of host strains for 15 passages (Fig. 1B, fig. S3), resulting in phage persistence even at high stringency under high dilution. The final BoNT/X variants converged on distinct combinations of mutations, with substitutions at N143, T167, and L364 independently enriched in all three replicates (Table S1). We observed a large apparent increase in Ykt6 selectivity in isolated variants (fig. S2), and characterized in depth clone BoNT/X(4130)B1 (Fig. 1D).

Purified X(4130)B1 protease (fig. S4) showed large increases in selectivity for Ykt6 over other native 60-mer substrate fragments when assayed *in vitro* (Fig. 1E–F) (55, 56). X(4130)B1 also showed reduced activity on not only VAMP1, but also other VAMP family substrates, despite the fact that no other VAMP homolog was the target of negative selection (Fig. 1F). Overall, evolved X(4130)B1 showed 1.5-fold higher activity on Ykt6 and 700-fold lower activity on VAMP1/2/3 relative to wild-type BoNT/X, representing a total evolved protease selectivity change of 1,060-fold. These findings establish that negative-selection protease PANCE can evolve variants of a promiscuous BoNT protease with greatly improved substrate selectivity.

Reversion analysis of X(4130)B1 demonstrated that A166E and T167I were responsible for much of the selectivity for Ykt6 over VAMP1 (fig. S5). We further obtained X-ray diffraction-quality crystals of X(4130)B1 protease, and solved the 1.8-Å resolution crystal structure (Fig. 2A, Table S2, PDB code 7KZ7). The fold of BoNT/X(4130)B1 is largely unchanged from that of wild-type BoNT/X LC (PDB code 6G47, rmsd=0.42 Å) (54). The

E166 mutation places a negatively charged Glu side chain across the active site cleft from the catalytic zinc cofactor. The structure of the related BoNT/F protease bound to a VAMP2 substrate mimic (40) suggests that E166 may interact with the substrate's P3 residue (Fig. 2A). We speculate that the A166E mutation electrostatically repels the anionic P3 residue (D66) in VAMP1, while tolerating the neutral P3 amino acid (V171) in Ykt6, thereby contributing to Ykt6 selectivity.

Negative-selection PANCE to evolve a VAMP4-selective BoNT/X protease

Next, we applied the protease negative selection to evolve BoNT/X LC into a VAMP4-selective protease that rejects VAMP1 (Fig. 1B, bottom). We began with PANCE in triplicate, again using a mutagenized population of wild-type BoNT/X phage, and observed phage titers drop rapidly at all stringencies, necessitating mutagenic drift at passage 5. After this re-diversification, phage began to persist at low dilution factors and under the lowest negative-selection stringency. Phage isolated after nine total passages converged on distinct sets of mutations between replicates, with mutations at N143, N164, P174, and S240 enriching across multiple populations. These proteases showed increased selectivity for VAMP4 over VAMP1 in the bacterial luciferase assay (fig. S6), although they also showed high apparent activity on Ykt6, likely because positions of divergence between VAMP1 and VAMP4 are mostly conserved between VAMP4 and Ykt6 (Fig. 1C).

We reinitiated PANCE using the same host strains to improve the partially VAMP4-selective phage. After 12 passages, clones from the highest stringency conditions in all three replicates (Fig. 1B, fig. S7) independently converged on mutations T224I and S240K (Table S3). The replicate that evolved the clones with the highest selectivity (*vide infra*) also converged on the A166E mutation present in the Ykt6-selective X(4130). Since VAMP4 similarly lacks a negatively charged P3 Asp, these results support the hypothesis that the A166E mutation provides selectivity against VAMP1.

When evaluated by luciferase assay, all variants from the final PANCE passage showed very high apparent selectivity for VAMP4 over VAMP1 (fig. S8). As with the X(4130)B1 protease, we observed selectivity for VAMP4 over all other natural BoNT/X substrates, including VAMP5 and Ykt6, in several evolved BoNT/X protease variants (fig. S8). Protease BoNT/X(5010)B1, which contained seven mutations relative to wild-type BoNT/X protease, exhibited the highest selectivity for VAMP4 over all other BoNT/X substrates (Fig. 1G) and was characterized further. X(5010)B1 contained mutations in the substrate-binding cleft that contribute to selectivity, including A166E, N164S, and P174T (fig. S9). Isolated X(5010)B1 protease (fig. S4) showed a 85-fold reduction in k_{cat}/K_M for VAMP1, and a 2.5-fold increase in k_{cat}/K_M for VAMP4, resulting in an overall catalytic efficiency (k_{cat}/K_M) change of 218-fold compared with wild-type BoNT/X protease. A substrate analysis revealed that X(5010)B1's preference for VAMP4 over VAMP5 improved >6-fold, and for VAMP4 over Ykt6 increased 2.8-fold (Fig. 1G). These outcomes establish the ability of the PANCE dual positive- and negative-selection system to evolve selective proteases.

Biological evaluation of evolved BoNT/X proteases

To further validate the selectivity and activity of the evolved BoNT/X proteases on full-length substrates, we incubated purified proteases with lysate from human HEK293T cells expressing full-length VAMP2, VAMP4, or Ykt6. In HEK293T cell lysates, X(4130)B1 and X(5010)B1 each cleave their respective new targets with selectivities consistent with their activity *in vitro* relative to wild-type BoNT/X protease (Fig. 1F–G, 2B).

To test if the evolved proteases remain compatible with native BoNT holotoxin delivery machinery, we incorporated proteases X(4130)B1 and X(5010)B1 into a hybrid holotoxin consisting of the evolved BoNT/X proteases linked to the BoNT/X translocation domain (H_N) and conjugated to the BoNT/A receptor-binding domain (H_C) via sortase-mediated ligation (53). This process generated chimeric holotoxins containing X(4130)B1 or X(5010)B1 as their LCs (fig. S10). Both of these evolved protease holotoxins showed potent self-delivery and efficient cleavage of their intended intracellular targets at picomolar concentrations in rat cortical neurons (Fig. 2C). Moreover, the evolved protease holotoxins show dramatically reduced (~100-fold lower) cleavage of their native target VAMP2, indicating that the large activity and selectivity changes evolved during PANCE in bacteria also manifest in neurons. These findings establish that the dual-selection protease evolution platform can generate reprogrammed BoNT proteases that support assembly into holotoxins, intracellular delivery into neurons, and selective activity on their chosen targets in mammalian cells.

Evolution of BoNT protease activity on a non-canonical SNARE substrate

We next challenged the dual selection system to reprogram a BoNT protease to cleave a novel SNARE target not known to be processed by any native BoNT protease. We chose to evolve BoNT/F LC protease due to the availability of structural (40) and structure-activity relationship (57) data. We selected the longin-SNARE VAMP7 as the target because of its role in trafficking, secretion, and autophagy (58). VAMP7 poses a challenge as a new target due to its limited homology (40% identity) with VAMP1/2/3 across the protease recognition site (Fig. 3A, bottom) (57), and no BoNT proteases have been reported to cleave VAMP7.

We designed a positive-selection evolutionary trajectory for BoNT/F protease starting from VAMP1(T29–K89) and ending with VAMP7(K121–R180) (Table S4). The trajectory passes through five intermediate substrates that serve as evolutionary stepping-stones (Fig. 3A). We first evolved tolerance of the D58G mutation in VAMP1 (stepping-stone F1, or SS.F1), which is known to prevent cleavage by BoNT/F (57). We then divided the surviving phage into three replicate populations that were subjected to PACE on the remaining stepping-stones in parallel to preserve access to diverse solutions (42). We added substrate mutations L55A (SS.F2), Q60E (SS.F3), and K61R (SS.F4) before challenging the surviving phage on SS.F7, which contained seven mutations as well as substrate termini from VAMP7 (Fig. 3A, bottom). Surviving phage were finally evolved in host cells harboring a T7-PAP containing VAMP7(K121–R180). The resulting replicate populations were pooled, then competed in a PACE experiment with a high-stringency VAMP7 AP, yielding the genotypes in Table S5.

The overall PACE campaign consisted of 795 hours of PACE in the longest linear path, requiring phage to survive an average total dilution of ~10^{240}-fold. The resulting proteases (Fig. 3B) exhibited high apparent cleavage activity on the VAMP7 selection substrate (Fig. 3C). One clone with 16 mutations relative to wild-type BoNT/F protease, F(3041)B6, showed 18-fold improved activity on VAMP7, constrained by the detection limit of VAMP7 cleavage by wild-type BoNT/F (fig. S11). These efforts generated the first protease to our knowledge that can cleave VAMP7, and the first example of a BoNT protease cleaving a protein outside the known substrate portfolio of natural BoNTs.

Consistent with prior efforts to reprogram proteases (19), the VAMP7-cleaving BoNT/F variants maintained activity on the native VAMP1 substrate (fig. S12). We therefore applied the dual selection system to reduce activity on VAMP1 while maintaining activity on VAMP7. Starting with the F(3041) population, we initiated PANCE in separate replicates at four negative-selection stringencies (Fig. 3A). Initially, phage persisted only with the two lowest-stringency negative-selection VAMP1 APs. After periodic reinfection into high-stringency negative-selection host cells, the evolving phage eventually accessed solutions that propagated in high-stringency host cells at 10-fold higher dilution levels than initial passages (fig. S13). After 15 total passages, we evaluated clones (Table S6) surviving the highest negative-selection stringency by luciferase assay (Fig. 3C). These assays suggested variants evolved greatly reduced activity on VAMP1, while maintaining VAMP7 activity. Based on activity, selectivity, and protein production levels, we selected BoNT/F(3230)A3 for in-depth characterization.

Purification and *in vitro* assessment confirmed that F(3230)A3 protease cleaves the target VAMP7 sequence (fig. S4, S14), with only trace cleavage of VAMP1 (Fig. 3D). Because the activity of wild-type BoNT/F on VAMP7 was too low to determine k_{cat}/K_M, turnover frequency (kcat,app) at 5 mM substrate was used to compare selectivity between evolved and wild-type BoNT/F proteases. The evolved F(3230)A3 protease cleaved VAMP1 (T29–K89) with a $k_{cat,app}$ of 1.6×10^{-4} s^{-1} and VAMP7 with a $k_{cat,app}$ of 7.7×10^{-3} s^{-1}. In contrast, wild-type BoNT/F protease cleaved VAMP1 with a $k_{cat,app}$ of 1.1 s^{-1} and VAMP7 with a $k_{cat,app}$ of 1.5×10^{-4} s^{-1}. Thus, the total selectivity change of evolved F(3230)A3 favoring VAMP7 (51-fold) and disfavoring VAMP1 (6,800-fold) is 3.5×10^5-fold.

To illuminate the role of individual mutations, we separately reverted each of the 21 mutations in F(3230)A3 and assessed their relative VAMP1 and VAMP7 cleavage activities by luciferase assay (fig. S15). None of the individual reversion mutants recovered meaningful VAMP1 activity, demonstrating that the origins of selectivity cannot be attributed to any single mutation. Several reversions (H72Y, A106V, N148S, P158A, Y166S, H184N, G200E, S224I, and L240R) reduced apparent VAMP7 activity, suggesting that they are important either for VAMP7 activity or for expression in *E. coli.* Four reversion mutations increased apparent VAMP7 activity: S232A, G350S, M381L, and L410P. When these four reversions were combined, VAMP1 off-target cleavage activity increased markedly (fig. S16). These results are consistent with the complex nature of BoNT protease substrate recognition and processing, driven by exosite binding interactions as well as conformational reorientation (39, 40).

BoNT/F(3230)A3 also demonstrated 20-fold selectivity for VAMP7 over all eight related VAMP family members (Table S7). While the basis of this broad selectivity is not clear, we determined by mass spectrometry that F(3230)A3 cleaved VAMP7 not between E153-N154 as anticipated, but instead nine residues C-terminal, after E162 (Fig. 3A bottom, fig. S17). This region of VAMP7 contains several residues, including L156, I158, T161, and N163, that are minimally conserved among the eight other VAMP family proteins. To test whether this cleavage site shift contributes to specificity for VAMP7, we generated chimeric VAMP7-VAMP1 substrates that substituted corresponding VAMP7 residues into VAMP1 at positions E64, D66, A69, and A71 (fig. S18). While none of the resulting individual VAMP1 mutants are competent substrates for F(3230)A3, the combination of all four substitutions yielded a substrate that was cleaved by evolved F(3230)A3 (fig. S18). These findings suggest that PACE evolved recognition of an optimal VAMP7 sequence that diverges from other VAMP homologs to survive the dual selection, resulting in broad specificity among other VAMP proteins.

Evolution of BoNT proteases that selectively cleave a non-SNARE target

To further challenge this protease evolution platform, we sought to generate BoNT proteases that selectively cleave a target unrelated to SNARE proteins. We selected BoNT/E protease for this purpose, which natively targets SNAP-25. Interactions between BoNT/E and SNAP-25 residues G168 (P13), D172 (P9), I178 (P3), and I181 (P1') are known important substrate recognition elements (59). We performed a protein BLAST search for targets that preserved these residues with similar spacing, with no restrictions on the 16 remaining positions across a nominal 20-residue cleavage site. We manually reviewed the resulting candidates for target sequence accessibility with available structural data, and for potential biomedical impact. This evaluation identified phosphatase and tensin homolog (PTEN) as an attractive target. PTEN plays a number of critical roles in cellular signaling (60, 61) and has been a target of longstanding interest in regenerative medicine. Recent reports suggest that PTEN knockdown can stimulate nerve regeneration after injury (62). PTEN is not a SNARE protein and shares only 4 of 20 residues with SNAP-25 flanking the anticipated proteolysis site. The evolution of a BoNT protease that selectively cleaves PTEN thus represents a formidable challenge.

Integrating the lessons from the campaigns described above, we pursued parallel evolutionary trajectories towards a PTEN-cleaving BoNT/E variant (Fig. 4A, Table S8). Trajectory A began by challenging proteases to recognize the P1 site R180S mutation (SS.E1a), starting from phage containing NNK codon randomization at E159 and N161 in BoNT/E. Survivors of PACE on SS.E1a were then challenged to cleave a stepping-stone substrate containing the D179C+R180S double mutant (SS.E2) either with continuous mutagenesis (Trajectory A1) or with NNK codon randomization of H216 and K225 prior to inoculation (Trajectory A2). Trajectory B began with the P2 site D179C mutation (SS.E1b), and PACE experiments were inoculated with BoNT/E phage carrying NNK codon libraries at H216 and K225. This initial PACE stage was also followed by selection on the D179C +R180S double mutant (SS.E2), either directly (Trajectory B1) or with NNK codon randomization of E159 and N161 (Trajectory B2) (Fig. 4A).

These PACE trajectories each converged on distinct genotypes. We evolved the resulting populations separately on four additional evolutionary stepping-stones before selection on the final PTEN target sequence (Fig. 4A–B). These intermediate substrates first incorporated PTEN residues S294–C296 in place of the SNAP-25 residues N169–N171 (SS.E3), then replaced the entire N-terminal SNAP-25 M167-Q177 with PTEN residues N292–S302 (SS.E4). Finally, all lineages were challenged with PACE on PTEN N292–N311 (AP-PTEN) at low then moderate stringency (Fig. 4A). Surviving phage originated from a single lineage (trajectory A1), which strongly enriched 10 consensus mutations relative to wild-type BoNT/E protease (Fig. 4C). In luciferase assays, the consensus clone E(0285)B6 demonstrated clear but weak PTEN cleavage activity (Fig. 4D, fig. S19). As expected given the absence of negative selection, this evolved protease retained high activity on its native SNAP-25 substrate.

Next, we performed low-stringency dual positive- and negative-selection PACE to reduce activity on SNAP-25 and improve activity on PTEN. These experiments evolved BoNT/E protease variants such as E(0308)B2 (Fig. 4C) with improved, but incomplete, selectivity (Fig. 4D). After rediversifying the protease populations across 15 passages of positive-selection PANCE on PTEN (Fig. 4A. middle bottom), we performed an additional 15 PANCE passages of dual positive and negative selection (Fig. 4A, fig. S20). After passage 15, phage from the host cells containing the highest stringency negative-selection APs (Table S9) converged on additional mutations C26Y, D156N, N248K, and Y357F (Fig. 4C). The consensus clone BoNT/E(4130)A2 carried 16 total mutations compared to wild-type BoNT/E protease, with seven mutations arising during negative selection. This E(4130)A2 protease demonstrated high apparent activity on the PTEN substrate with nearly undetectable activity on SNAP-25 in luciferase assays (Fig. 4D). Reversion analysis (fig. S21) revealed that E159L, N161N, Q162S, and R163S contribute to PTEN cleavage activity.

Isolation and *in vitro* kinetic assessment of E(4130)A2 (fig. S4) confirmed high activity levels on PTEN and low activity on SNAP-25. E(4130)A2 protease efficiently cleaved the target PTEN sequence, which is not detectably cleaved by wild-type BoNT/E protease, with a measured improvement in k_{cat} of >18,300-fold, constrained by the assay's limit of detection (Fig. 4E). When combined with 606-fold reduced cleavage of the endogenous SNAP-25 substrate (Fig. 4E), E(4130)A2 exhibits an overall 1.1×10^7-fold change in substrate selectivity. This large change in selectivity was driven primarily by a much higher k_{cat} for PTEN, which increased from $<3.2 \times 10^{-5}$ s^{-1} for wild-type BoNT/E protease to 0.59 s^{-1} for E(4130)A2, rather than by an impaired K_M for SNAP-25 (fig. S22). Selectivity through k_{cat} rather than K_M is consistent with host cells producing a large excess of off-target SNAP-25 substrate relative to the on-target substrate during the negative selection. At high concentrations of SNAP-25, BoNT/E variants that evolve impaired K_M for SNAP-25 likely gain little fitness compared to variants that evolve impaired k_{cat} for SNAP-25. Adjusting the concentrations of substrates (PAPs) could modify the selection in ways that favor improvements in selectivity that are K_M-driven.

Interestingly, the E(4130)A2 cleavage site in PTEN was determined by mass spectrometry to occur after PTEN residue S302 (fig. S23), three residues N–terminal from our predicted cleavage position. This cleavage position preserves key amino acid identity between

SNAP-25 and PTEN at P1', P2, and P3, which is apparently preferred over predicted cleavage site preservation at P1', P3, P9, and P13 (Fig. 4B). Consistent with the cleavage site shift during the evolution of BoNT/F(3230)A3, positional flexibility during protease evolution may contribute to the acquisition of selective activity on new targets. Collectively, these results represent the first example of generating a BoNT protease that cleaves a non-SNARE substrate.

Finally, we assessed E(4130)A2 in mammalian cells. We co-transfected plasmids encoding the protease and PTEN into human HEK293T cells. Although weak cleavage of PTEN was detected, most PTEN was not cleaved in cells (Fig. 4F), potentially because PTEN is localized to plasma membranes, while BoNT/E LC is known to remain cytosolic (63). To localize the evolved protease to plasma membranes, we fused to the N-terminus of E(4130)A2 a plextrin homology (PH) domain from protein kinase C that binds to plasma membranes (64). Co-expression of this PH-E(4130)A2 protease with full-length PTEN resulted in efficient cleavage in HEK293 cells (Fig. 4F). Expression of either E(4130)A2 or PH-E(4130)A2 resulted in no loss of viability (fig. S24), an important additional indicator of selectivity.

We also transduced rat cortical neurons with lentivirus encoding PH-E(4130)A2, and examined cleavage of both endogenous PTEN and SNAP-25 by western blot. The transduced cells show substantial cleavage of endogenous PTEN, with minimal off-target cleavage of the native BoNT/E substrate SNAP-25 (Fig. 4G). This selectivity was further enhanced by introducing the L166A mutation, which is known to disrupt an exosite binding interaction and decrease SNAP-25 cleavage by BoNT/E protease (65) (Fig. 4G). Other endogenous SNARE proteins such as VAMP2 and Syntaxin 1 were not cleaved by PH-E(4130)A2 (Fig. 4G). These results confirm that evolved BoNT proteases emerging from dual-selection PACE can support efficient and selective proteolysis of a non-SNARE target in mammalian cells.

Discussion

Botulinum neurotoxins are powerful agents for mediating intracellular proteolysis, but attempts to extend their application beyond their small set of native SNARE protein targets has been a longstanding challenge. Here we developed and applied a dual-selection PACE system to evolve four BoNT protease variants that selectively cleave both native (Ykt6, VAMP4) and non-native (VAMP7, PTEN) substrates. The efficiency of phage-assisted evolution enables complex fitness landscapes to be quickly navigated using parallel trajectories and carefully controlled positive- and negative-selection stringencies. This system makes practical the evolution of proteases over hundreds of generations of mutation, selection, and replications. Varying additional selection parameters such as substrate concentration and PAP efficiency could in principle generate proteases with additional desired properties.

Our findings establish that BoNT proteases may be far more evolutionarily malleable than their high natural target specificity would suggest. The evolved F(3230)A3 and E(4130)A2 proteases cleave new substrates that share limited homology with their native substrates. The

known exosite dependence of BoNT proteases may facilitate reprogramming their specificities, since their extended enzyme-substrate interface provides a large surface over which new contacts can evolve while maintaining interactions required for catalysis.

Though extended substrate recognition may contribute evolutionary plasticity and selectivity in BoNT proteases, we found a structurally homologous 5-amino acid stretch of BoNT protease active sites (residues 164–168 in BoNT/F, 159–163 in BoNT/E, and 164–168 in BoNT/X) that carried at least two mutations in each of the evolved proteases characterized in depth in this study (fig. S25). The comparatively high frequency of mutations in this region across all four evolved proteases suggests that diversifying this region of BoNT proteases may be especially productive for future BoNT reprogramming efforts.

The ability to potently deliver their protease domains to the cytosol of susceptible cells is a remarkable feature of BoNTs. It is encouraging that evolved BoNT proteases can retain compatibility with translocation machinery in BoNT HCs to form functional holotoxins. Efforts to engineer BoNT HCs to support self-delivery to various cell and tissue types (66) raise the intriguing possibility of developing evolved BoNTs for tissue-specific delivery of reprogrammed proteases that selectively manipulate target intracellular proteins.

Supplementary Material

Refer to Web version on PubMed Central for supplementary material.

Acknowledgments:

## References and Notes

1. Li Q, Yi L, Marek P, Iverson BL, Commercial proteases: present and future. FEBS Lett 587, 1155–1163 (2013). [PubMed: 23318711]

2. Zhao H, Arnold FH, Directed evolution converts subtilisin E into a functional equivalent of thermitase. Protein Engineering, Design and Selection 12, 47–53 (1999).

3. You L, Arnold FH, Directed evolution of subtilisin E in Bacillus subtilis to enhance total activity in aqueous dimethylformamide. Protein Eng 9, 77–83 (1996). [PubMed: 9053906]

4. Madison EL, Goldsmith EJ, Gerard RD, Gething MJ, Sambrook JF, Serpin-resistant mutants of human tissue-type plasminogen activator. Nature 339, 721–724 (1989). [PubMed: 2500599]

5. Dickinson BC, Packer MS, Badran AH, Liu DR, A system for the continuous directed evolution of proteases rapidly reveals drug-resistance mutations. Nat Commun 5, 5352 (2014). [PubMed: 25355134]

6. Meister SW, Hendrikse NM, Lofblom J, Directed evolution of the 3C protease from coxsackievirus using a novel fluorescence-assisted intracellular method. Biol Chem 400, 405–415 (2019). [PubMed: 30521472]

7. Sanchez MI, Ting AY, Directed evolution improves the catalytic efficiency of TEV protease. Nat Methods 17, 167–174 (2020). [PubMed: 31819267]

8. Allen GA et al., A variant of recombinant factor VIIa with enhanced procoagulant and antifibrinolytic activities in an in vitro model of hemophilia. Arterioscler Thromb Vasc Biol 27, 683–689 (2007). [PubMed: 17204663]

9. Sellamuthu S et al., Engineering of protease variants exhibiting altered substrate specificity. Biochem Biophys Res Commun 371, 122–126 (2008). [PubMed: 18413229]

10. Tran DT, Cavett VJ, Dang VQ, Torres HL, Paegel BM, Evolution of a mass spectrometry-grade protease with PTM-directed specificity. Proc Natl Acad Sci U S A 113, 14686–14691 (2016). [PubMed: 27940920]

11. Sidhu SS, Borgford TJ, Selection of Streptomyces griseus protease B mutants with desired alterations in primary specificity using a library screening strategy. J Mol Biol 257, 233–245 (1996). [PubMed: 8609620]

12. Renicke C, Spadaccini R, Taxis C, A tobacco etch virus protease with increased substrate tolerance at the P1' position. PLoS One 8, e67915 (2013). [PubMed: 23826349]

13. Verhoeven KD, Altstadt OC, Savinov SN, Intracellular detection and evolution of site-specific proteases using a genetic selection system. Appl Biochem Biotechnol 166, 1340–1354 (2012). [PubMed: 22270548]

14. Lin YC et al., Alteration of substrate and inhibitor specificity of feline immunodeficiency virus protease. J Virol 74, 4710–4720 (2000). [PubMed: 10775609]

15. Ridky TW et al., Programming the Rous sarcoma virus protease to cleave new substrate sequences. J Biol Chem 271, 10538–10544 (1996). [PubMed: 8631853]

16. Sellamuthu S et al., An engineered viral protease exhibiting substrate specificity for a polyglutamine stretch prevents polyglutamine-induced neuronal cell death. PLoS One 6, e22554 (2011). [PubMed: 21799895]

17. Guerrero JL, O'Malley MA, Daugherty PS, Intracellular FRET-based Screen for Redesigning the Specificity of Secreted Proteases. ACS Chem Biol 11, 961–970 (2016). [PubMed: 26730612]

18. Hill ME et al., Reprogramming Caspase-7 Specificity by Regio-Specific Mutations and Selection Provides Alternate Solutions for Substrate Recognition. ACS Chem Biol 11, 1603–1612 (2016). [PubMed: 27032039]

19. Packer MS, Rees HA, Liu DR, Phage-assisted continuous evolution of proteases with altered substrate specificity. Nat Commun 8, 956 (2017). [PubMed: 29038472]

20. Dorr BM, Ham HO, An C, Chaikof EL, Liu DR, Reprogramming the specificity of sortase enzymes. Proc Natl Acad Sci U S A 111, 13343–13348 (2014). [PubMed: 25187567]

21. Carlson JC, Badran AH, Guggiana-Nilo DA, Liu DR, Negative selection and stringency modulation in phage-assisted continuous evolution. Nat Chem Biol 10, 216–222 (2014). [PubMed: 24487694]

22. Badran AH et al., Continuous evolution of Bacillus thuringiensis toxins overcomes insect resistance. Nature 533, 58–63 (2016). [PubMed: 27120167]

23. Hu JH et al., Evolved Cas9 variants with broad PAM compatibility and high DNA specificity. Nature 556, 57–63 (2018). [PubMed: 29512652]

24. Esvelt KM, Carlson JC, Liu DR, A system for the continuous directed evolution of biomolecules. Nature 472, 499–503 (2011). [PubMed: 21478873]

25. Santoro SW, Wang L, Herberich B, King DS, Schultz PG, An efficient system for the evolution of aminoacyl-tRNA synthetase specificity. Nat Biotechnol 20, 1044–1048 (2002). [PubMed: 12244330]

26. Levin KB et al., Following evolutionary paths to protein-protein interactions with high affinity and selectivity. Nat Struct Mol Biol 16, 1049–1055 (2009). [PubMed: 19749752]

27. Renata H, Wang ZJ, Arnold FH, Expanding the enzyme universe: accessing non-natural reactions by mechanism-guided directed evolution. Angew Chem Int Ed Engl 54, 3351–3367 (2015). [PubMed: 25649694]

28. Carrico ZM, Strobel KL, Atreya ME, Clark DS, Francis MB, Simultaneous selection and counter-selection for the directed evolution of proteases in E. coli using a cytoplasmic anchoring strategy. Biotechnol Bioeng 113, 1187–1193 (2016). [PubMed: 26666461]

29. Varadarajan N, Gam J, Olsen MJ, Georgiou G, Iverson BL, Engineering of protease variants exhibiting high catalytic activity and exquisite substrate selectivity. Proc Natl Acad Sci U S A 102, 6855–6860 (2005). [PubMed: 15867160]

30. Varadarajan N, Rodriguez S, Hwang BY, Georgiou G, Iverson BL, Highly active and selective endopeptidases with programmed substrate specificities. Nat Chem Biol 4, 290–294 (2008). [PubMed: 18391948]

31. Yi L et al., Engineering of TEV protease variants by yeast ER sequestration screening (YESS) of combinatorial libraries. Proc Natl Acad Sci U S A 110, 7229–7234 (2013). [PubMed: 23589865]

32. Varadarajan N, Georgiou G, Iverson BL, An engineered protease that cleaves specifically after sulfated tyrosine. Angew Chem Int Ed Engl 47, 7861–7863 (2008). [PubMed: 18780393]

33. Ramesh B et al., Engineered ChymotrypsiN for Mass Spectrometry-Based Detection of Protein Glycosylation. ACS Chem Biol 14, 2616–2628 (2019). [PubMed: 31710461]

34. Dong M, Masuyer G, Stenmark P, Botulinum and Tetanus Neurotoxins. Annu Rev Biochem 88, 811–837 (2019). [PubMed: 30388027]

35. Pirazzini M, Rossetto O, Eleopra R, Montecucco C, Botulinum Neurotoxins: Biology, Pharmacology, and Toxicology. Pharmacol Rev 69, 200–235 (2017). [PubMed: 28356439]

36. Sudhof TC, Rothman JE, Membrane fusion: grappling with SNARE and SM proteins. Science 323, 474–477 (2009). [PubMed: 19164740]

37. Chen S, Barbieri JT, Engineering botulinum neurotoxin to extend therapeutic intervention. Proc Natl Acad Sci U S A 106, 9180–9184 (2009). [PubMed: 19487672]

38. Binz T et al., Mutations in light chain of botulinum neurotoxin a enable cleavage of human SNAP-23. . Toxicon 156, S10 (2018).

39. Breidenbach MA, Brunger AT, Substrate recognition strategy for botulinum neurotoxin serotype A. Nature 432, 925–929 (2004). [PubMed: 15592454]

40. Agarwal R, Schmidt JJ, Stafford RG, Swaminathan S, Mode of VAMP substrate recognition and inhibition of Clostridium botulinum neurotoxin F. Nat Struct Mol Biol 16, 789–794 (2009). [PubMed: 19543288]

41. Guerrero JL, Daugherty PS, O'Malley MA, Emerging technologies for protease engineering: New tools to clear out disease. Biotechnol Bioeng 114, 33–38 (2017). [PubMed: 27497426]

42. Dickinson BC, Leconte AM, Allen B, Esvelt KM, Liu DR, Experimental interrogation of the path dependence and stochasticity of protein evolution using phage-assisted continuous evolution. Proc Natl Acad Sci U S A 110, 9007–9012 (2013). [PubMed: 23674678]

43. Hubbard BP et al., Continuous directed evolution of DNA-binding proteins to improve TALEN specificity. Nat Methods 12, 939–942 (2015). [PubMed: 26258293]

44. Badran AH, Liu DR, Development of potent in vivo mutagenesis plasmids with broad mutational spectra. Nat Commun 6, 8425 (2015). [PubMed: 26443021]

45. Bryson DI et al., Continuous directed evolution of aminoacyl-tRNA synthetases. Nat Chem Biol 13, 1253–1260 (2017). [PubMed: 29035361]

46. Roth TB, Woolston BM, Stephanopoulos G, Liu DR, Phage-Assisted Evolution of Bacillus methanolicus Methanol Dehydrogenase 2. ACS Synth Biol 8, 796–806 (2019). [PubMed: 30856338]

47. Richter MF et al., Phage-assisted evolution of an adenine base editor with improved Cas domain compatibility and activity. Nat Biotechnol 38, 883–891 (2020). [PubMed: 32433547]

48. Miller SM et al., Continuous evolution of SpCas9 variants compatible with non-G PAMs. Nat Biotechnol 38, 471–481 (2020). [PubMed: 32042170]

49. Thuronyi BW et al., Continuous evolution of base editors with expanded target compatibility and improved activity. Nat Biotechnol 37, 1070–1079 (2019). [PubMed: 31332326]

50. Miller SM, Wang T, Liu DR, Phage-assisted continuous and non-continuous evolution. Nat Protoc 15, 4101–4127 (2020). [PubMed: 33199872]

51. Masuyer G, Chaddock JA, Foster KA, Acharya KR, Engineered botulinum neurotoxins as new therapeutics. Annu Rev Pharmacol Toxicol 54, 27–51 (2014). [PubMed: 24016211]

52. Keith F, John C, Targeted secretion inhibitors-innovative protein therapeutics. Toxins (Basel) 2, 2795–2815 (2010). [PubMed: 22069575]

53. Zhang S et al., Identification and characterization of a novel botulinum neurotoxin. Nat Commun 8, 14130 (2017). [PubMed: 28770820]

54. Masuyer G et al., Structural characterisation of the catalytic domain of botulinum neurotoxin X - high activity and unique substrate specificity. Sci Rep 8, 4518 (2018). [PubMed: 29540745]

55. Ruge DR et al., Detection of six serotypes of botulinum neurotoxin using fluorogenic reporters. Anal Biochem 411, 200–209 (2011). [PubMed: 21216216]

56. Dong M, Tepp WH, Johnson EA, Chapman ER, Using fluorescent sensors to detect botulinum neurotoxin activity in vitro and in living cells. Proc Natl Acad Sci U S A 101, 14701–14706 (2004). [PubMed: 15465919]

57. Sikorra S, Henke T, Galli T, Binz T, Substrate recognition mechanism of VAMP/synaptobrevin-cleaving clostridial neurotoxins. J Biol Chem 283, 21145–21152 (2008). [PubMed: 18511418]

58. Daste F, Galli T, Tareste D, Structure and function of longin SNAREs. J Cell Sci 128, 4263–4272 (2015). [PubMed: 26567219]

59. Chen S, Barbieri JT, Unique substrate recognition by botulinum neurotoxins serotypes A and E. J Biol Chem 281, 10906–10911 (2006). [PubMed: 16478727]

60. Lee YR, Chen M, Pandolfi PP, The functions and regulation of the PTEN tumour suppressor: new modes and prospects. Nat Rev Mol Cell Biol 19, 547–562 (2018). [PubMed: 29858604]

61. Worby CA, Dixon JE, Pten. Annu Rev Biochem 83, 641–669 (2014). [PubMed: 24905788]

62. Liu K et al., PTEN deletion enhances the regenerative ability of adult corticospinal neurons. Nat Neurosci 13, 1075–1081 (2010). [PubMed: 20694004]

63. Fernandez-Salas E et al., Plasma membrane localization signals in the light chain of botulinum neurotoxin. Proc Natl Acad Sci U S A 101, 3208–3213 (2004). [PubMed: 14982988]

64. Chen J, Chen ZJ, PtdIns4P on dispersed trans-Golgi network mediates NLRP3 inflammasome activation. Nature 564, 71–76 (2018). [PubMed: 30487600]

65. Chen S, Barbieri JT, Multiple pocket recognition of SNAP25 by botulinum neurotoxin serotype E. J Biol Chem 282, 25540–25547 (2007). [PubMed: 17609207]

66. Pickett A, Perrow K, Towards new uses of botulinum toxin as a novel therapeutic tool. Toxins (Basel) 3, 63–81 (2011). [PubMed: 22069690]

67. Otwinowski Z, Minor W, Processing of X-ray Diffraction Data Collected in Oscillation Mode. Methods in enzymology 276, 307–326 (1997).

68. Minor W, Cymborowski M, Otwinowski Z, Chruszcz M, HKL-3000: the integration of data reduction and structure solution--from diffraction images to an initial model in minutes. Acta Crystallogr D Biol Crystallogr 62, 859–866 (2006). [PubMed: 16855301]

69. Murshudov GN et al., REFMAC5 for the refinement of macromolecular crystal structures. Acta Crystallogr D Biol Crystallogr 67, 355–367 (2011). [PubMed: 21460454]

70. Morris RJ, Perrakis A, Lamzin VS, ARP/wARP and Automatic Interpretation of Protein Electron Density Maps. Methods in Enzymology 374, 229–244 (2003). [PubMed: 14696376]

71. Emsley P, Cowtan K, Coot: model-building tools for molecular graphics. Acta Crystallogr D Biol Crystallogr 60, 2126–2132 (2004). [PubMed: 15572765]

72. Painter J, Merritt EA, Optimal description of a protein structure in terms of multiple groups undergoing TLS motion. Acta Crystallogr D Biol Crystallogr 62, 439–450. (2006). [PubMed: 16552146]

73. Chen VB et al., MolProbity: all-atom structure validation for macromolecular crystallography. Acta Crystallogr D Biol Crystallogr 66, 12–21 (2010). [PubMed: 20057044]
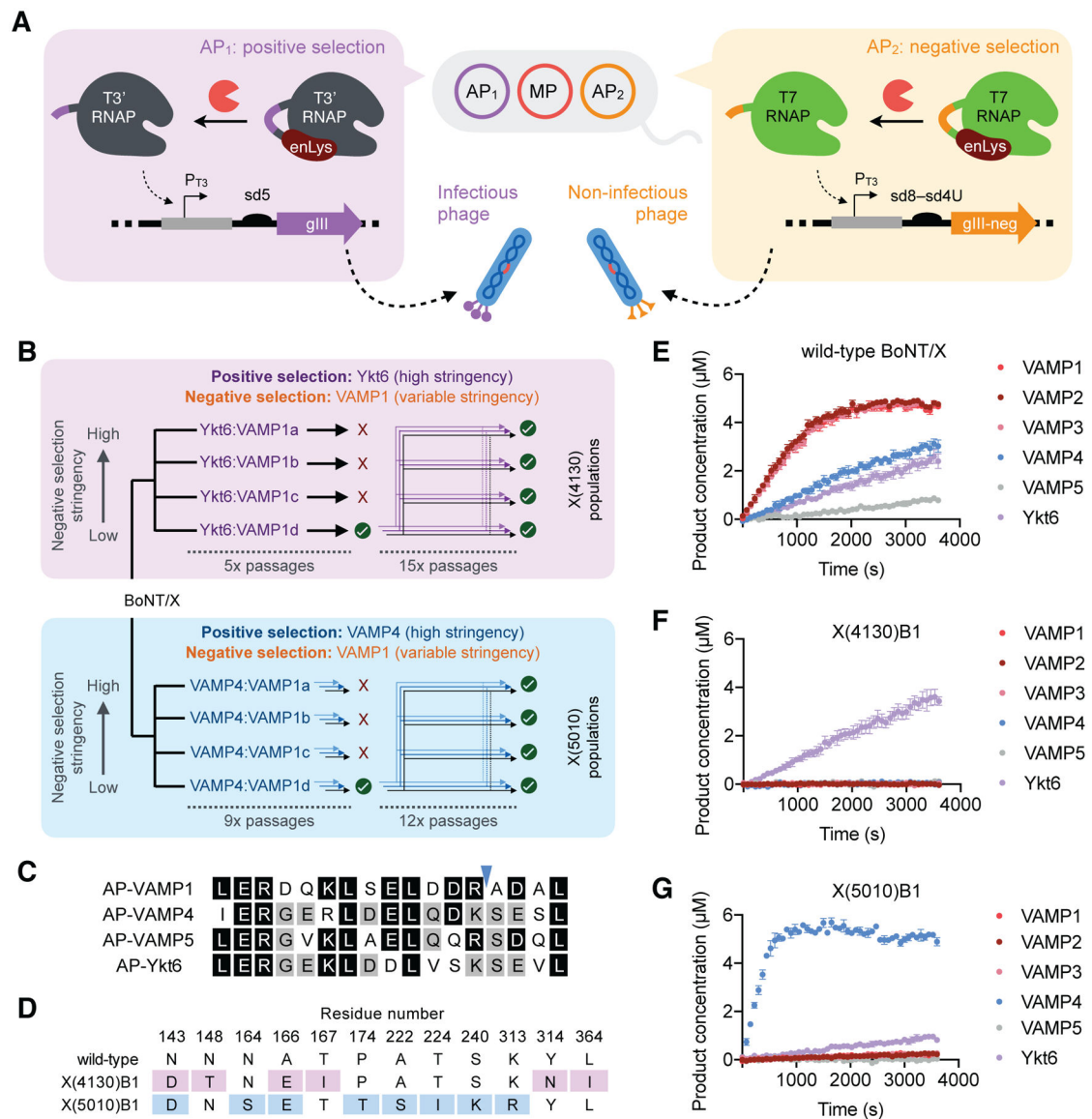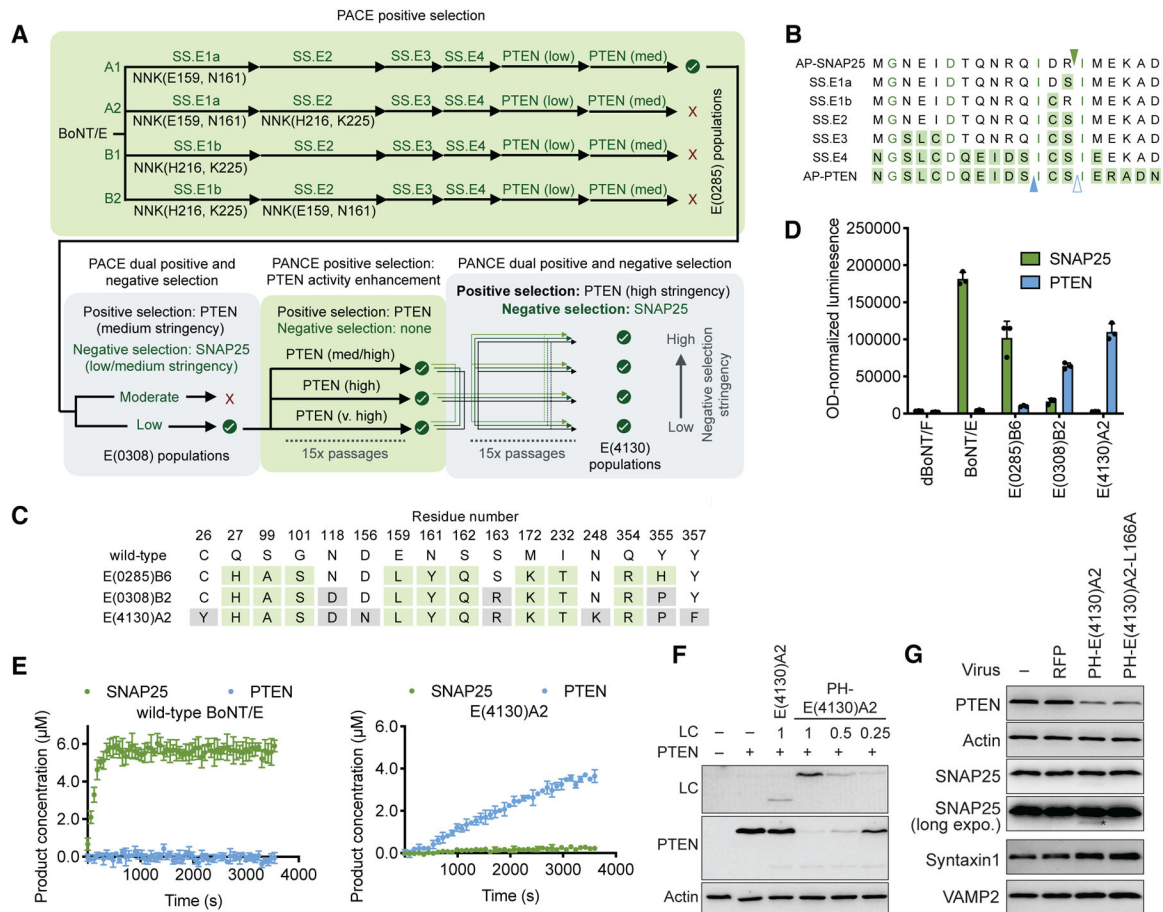
Figure 1.

(**A**) Schematic of the PACE/PANCE dual positive and negative selection for proteolysis. (**B**) Summary of the strategy for stepwise evolution of a Ykt6-selective and a VAMP4-selective protease from promiscuous wild-type BoNT/X LC protease. (**C**) Four major substrates of wild-type BoNT/X protease, with the cleavage position indicated by the blue wedge. Positions in VAMP4, VAMP5, and Ykt6 identical to VAMP1 are in black, while positions in VAMP5 and Ykt6 identical to VAMP4 are in grey. (**D**) Selected Ykt6-selective and VAMP4-selective BoNT/X protease variants. (**E-G**) Representative kinetic traces showing cleavage activity of wild-type BoNT/X protease, X(4130)B1 protease, and X(5101)B1 protease on the seven major BoNT/X substrates. Reactions in (E-G) were performed at 37 °C with 2.5 nM protease and 5 μM substrate.
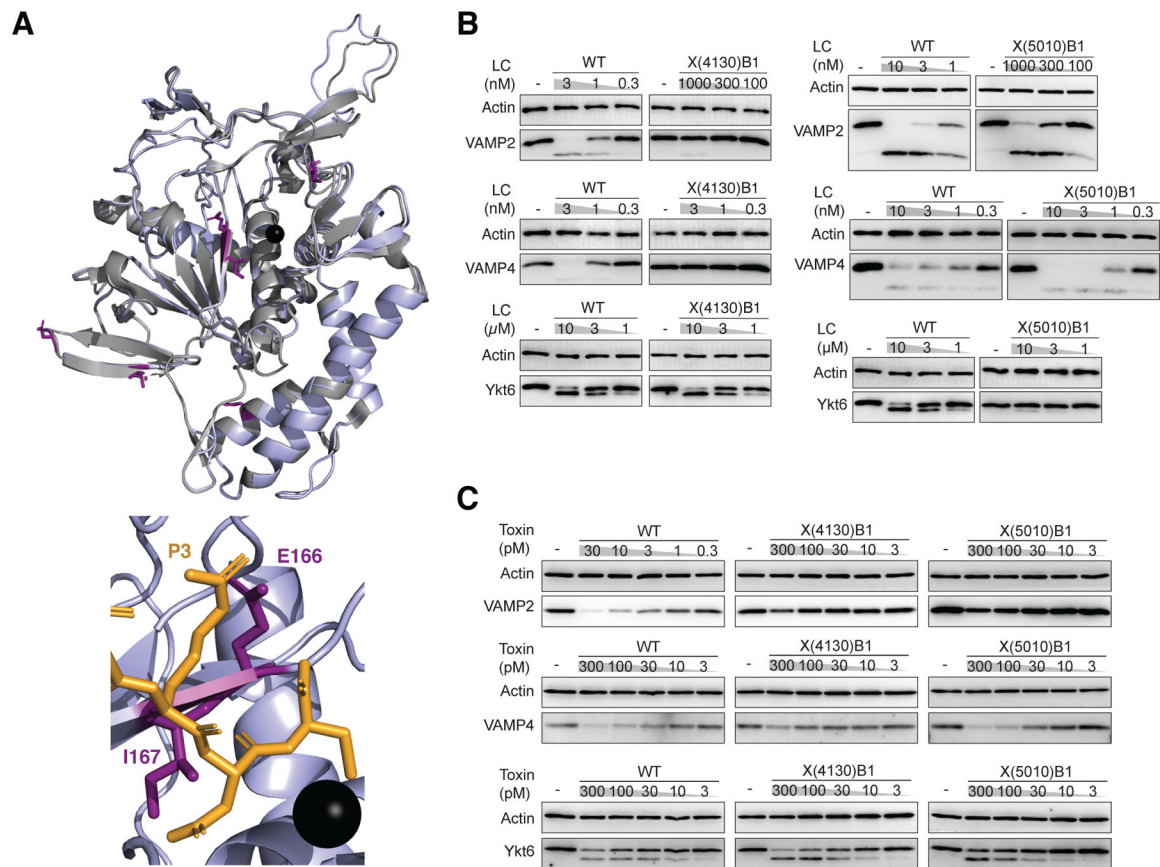
Figure 2.
(**A**) Top: Superposition of the 1.8-Å resolution x-ray crystal structure of evolved X(4130)B1 (light blue) with the wild-type BoNT/X LC (grey, PDB 6F4E). Mutated residues in X(4130)B1 are shown in purple, with the active site zinc shown as a black sphere. Bottom: Superposition of a BoNT/F LC-bound VAMP2-mimic (orange, from PDB 3FIE) and the crystal structure of X(4130)B1 (light blue), showing the close proximity of the P3 Arg (orange) to E166 and I167 (purple). The active site zinc is shown as a black sphere. (**B**) Evaluation of X(4130)B1 and X(5010)B1 activity on full-length substrates in human HEK293T cell lysates by immunoblot. Actin served as a loading control. (**C**) Evolved protease delivery and activity as chimeric BoNT holotoxins (53) added to cultured rat cortical neurons. Neurons were treated with the indicated concentration of holotoxin for 16 h. Cleavage on endogenous VAMP2, VAMP4, and Ykt6 was detected by immunoblot on neuron lysates.
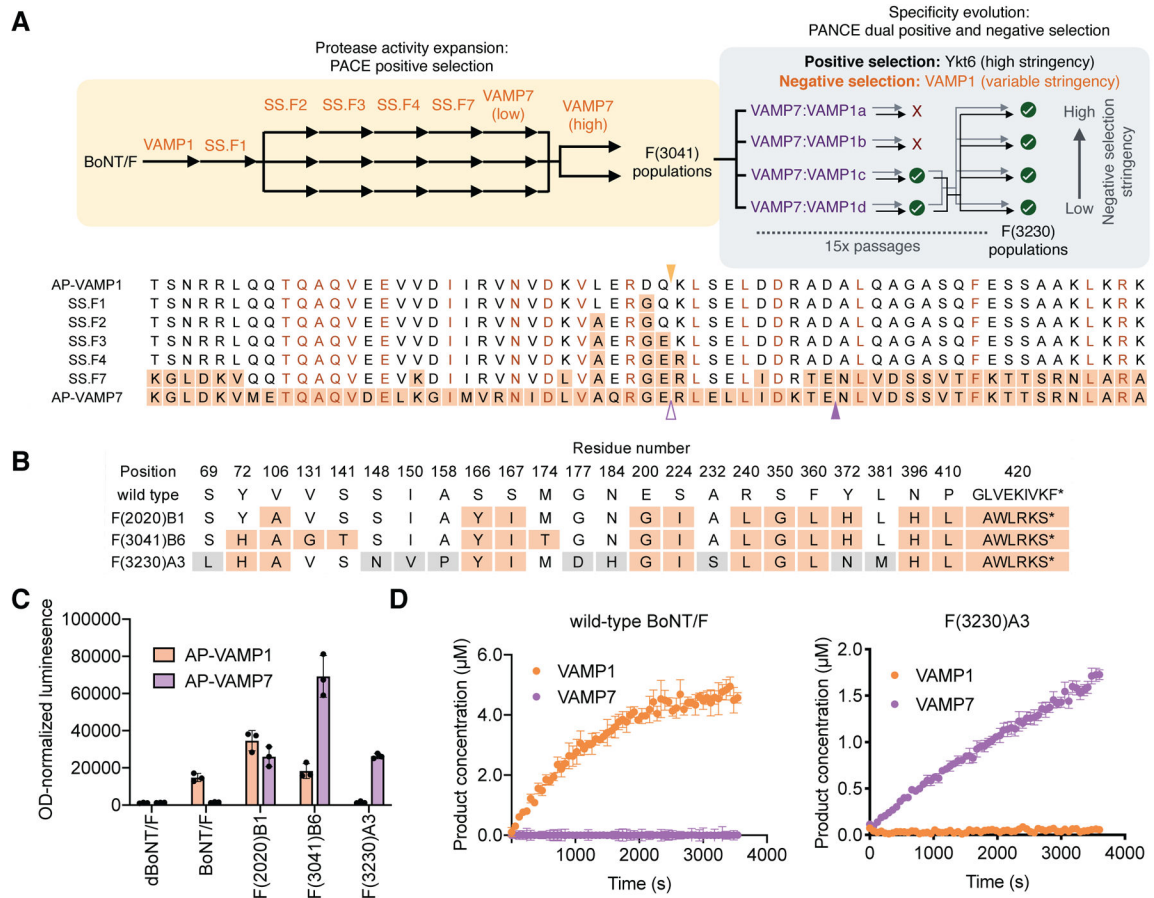
Figure 3.
(**A**) Top: Summary of the strategy for stepwise evolution of a VAMP7-cleaving protease from BoNT/F LC protease, followed by dual positive and negative selection for evolving VAMP7 selectivity from promiscuous variants. Bottom: substrates used during the evolution of a VAMP7-selective protease from a VAMP1-cleaving protease. The orange wedge shows the wild-type BoNT/F cleavage site. The predicted (hollow) and actual (filled) purple wedges show VAMP7 cleavage sites of the evolved F(3230)A3 protease. (**B**) Selected variants from evolution of VAMP7-selective BoNT/F proteases. Mutations in grey enriched during negative selection. (**C**) Apparent protease activity by luciferase assay for selected clones from various stages of BoNT/F evolution. (**D**) Comparison of wild-type BoNT/F protease (left) and evolved F(3230)A3 protease (right) activity on VAMP1 and VAMP7. Assays were performed using proteases containing an N-terminal MBP tag under standard assay conditions at 37 °C with 5 μM substrate and either 2.5 nM BoNT/F or 50 nM F(3230)A3.

Figure 4.
(**A**) Strategy for stepwise evolution of a PTEN-cleaving protease from wild-type SNAP-25-cleaving BoNT/E LC protease. (**B**) Protease cleavage substrates used during the evolution of a PTEN-selective protease. (**C**) Selected variants from the evolution of a PTEN-selective BoNT/E protease. Mutations in green enriched during the positive selection, and mutations in grey enriched during negative selection. (**D**) Apparent protease activity by luciferase assay of clones from BoNT/E evolution. dBoNT/F is an inactive BoNT/F protease mutant. (**E**) Comparison of wild-type BoNT/E LC (left) and E(4130)A2 protease (right) activity on SNAP25 and PTEN. Assays were performed under standard conditions at 37 °C using 5 μM substrate and 10 nM protease. (**F**) Evaluation of full-length PTEN cleavage in cells. FLAG-tagged full-length PTEN was co-expressed with either HA-tagged E(4130)A2 or HA-tagged PH-E(4130)A2 in HEK293 cells. PH-E(4130)A2 contains an N-terminal pleckstrin homology (PH) domain fused to E(4130)A2. Cell lysates were analyzed by immunoblot, detecting PTEN (via FLAG-tag) and E(4130)A2 (via HA tag). Actin served as a loading control. Numbers indicate the ratio of BoNT/LC plasmid:PTEN substrate plasmid. LC, light-chain proteases. (**G**) PTEN and SNARE protein cleavage in cultured rat cortical neurons transduced with lentivirus expressing RFP (negative control), PH-E(4130)A2 protease, or the PH-E(4130)A2(L166A) protease. Neuron lysates were analyzed by immunoblot, detecting endogenous PTEN, SNAP-25, VAMP2, and Syntaxin 1. Actin served as a loading control. The asterisk marks the minor cleavage of SNAP-25 by PH-E(4130)A2

detected with long exposure time (Long expo.), which is not observed for PH-E(4130)A2(L166A).